Available online at www.sciencedirect.com

ScienceDirect

IFAC Papers Online CONFERENCE PAPER ARCHIVE

IFAC PapersOnLine 51-28 (2018) 37–42

Frequency Control of Distributed Energy Resources in Distribution Networks ⋆

Álvaro Ortega * **Federico Milano** *

* *School of Electrical & Electronic Engineering*
University College Dublin, Ireland
(e-mails: alvaro.ortegamanjavacas@ucd.ie; federico.milano@ucd.ie.)

Abstract: This paper studies the contribution of distributed energy resources (DERs) installed in distribution systems to the frequency regulation of transmission systems. To this aim, the paper compares three strategies to retrieve the input signal of the DER frequency regulators, namely (i) measuring the frequency at the point of common coupling with the transmission system; (ii) measuring locally the frequency signals at every bus with regulation of the distribution system; and (iii) computing the average of such signals. The impact of measurement issues caused by the computation of the numerical derivative of the bus voltage phase angle, as well as of noise, delays and loss of information are also thoroughly analyzed in the case study.

Keywords: Primary frequency control, rate of change of frequency (RoCoF), distributed energy resource (DER), distribution systems, phase-locked loop (PLL), measurement delays.

1. INTRODUCTION

Until recent years, frequency regulation from distributed energy resources (DERs) such as wind turbines and solar photo-voltaic generation (SPVG) was not available, as they were operated with the aim of supplying their maximum feasible power according to meteorological conditions by means of the maximum power point tracking (MPPT) control [Ekanayake and Jenkins (2004); Tamimi et al. (2011)]. This situation is rapidly changing. As the penetration of DERs increases, in fact, there is the urgent need to maintain the system frequency regulation capability while the system inertia is being reduced. However, while active power curtailment is generally always available for wind turbines and SPVG in case of over-frequencies, they usually cannot guarantee a power reserve in case of under-frequencies. To overcome this issue, energy storage systems (ESSs) become apparent, thanks to their capability to supply/absorb large amounts of active and reactive power simultaneously in very short time frames [Ortega and Milano (2017a)].

While the provision of frequency control through DERs is considered to be inevitable, there is still no clear understanding on what is the best approach to control such devices [Ramtharan et al. (2007); Morren et al. (2006); Cerqueira et al. (2017); Tamimi et al. (2011)]. In particular, there are several concerns for DERs with "small" capacity, which are typically connected to the distribution (medium voltage) level. The main issues that are anticipated for the control of these DERs are: (i) large number of small devices; (ii) relatively high noise in the distribution network due to the proximity to loads.

The large number of devices suggests to adopt some kind of centralized control, which makes sure that the response of all devices is consistent and contributes to the stable operation of the systems. A sort of centralized control has been proposed in the so-called "virtual power plants" [Etherden et al. (2016); Koraki and Strunz (2018)]. A centralized control, however, is expected to introduce delays and communication issues which can significantly reduce the effectiveness of the control itself.

Conventional primary frequency control has been implemented in a decentralized way, also because typical power plants have a "good" local estimation of the frequency which is the rotor speed of the synchronous machines. Since DERs are typically non-synchronous, the frequency has to be estimated based on voltage/current phasors at the point of connection of the DER. This is done typically with a phase-locked loop (PLL) device, which unfortunately introduces errors, e.g., due to the calculation of the numerical derivative of phasor components. Reference [Ortega and Milano (2017b)] shows that the impact of PLLs on the frequency regulation of non-synchronous generation at the high-voltage transmission system level can create instabilities. Similar issues have to be anticipated for the frequency estimation of PLLs at the medium-voltage distribution system level.

This paper provides a comprehensive study on the impact of the frequency control of distribution-level DERs on the overall transient behavior of transmission systems. The paper proposes three strategies to generate the signal used as input of the DER frequency regulators: (i) decentralized, where each DER estimates its local frequency through a PLL; (ii) centralized, where the DERs connected to the same distribution system receive a common signal from a PLL installed at the point of contact of the distribution network with the transmission system; and (iii) average, where the frequency estimations of the DERs are collected

⋆ This material is based upon works funded by European Union's Horizon 2020 research and innovation programme under grant agreement N°727481. F. Milano is also funded by the Science Foundation Ireland, grant No. SFI/15/IA/3074.

10.1016/j.ifacol.2018.11.674

at the distribution system level and then a common, average signal is sent back to each DER. The case study also duly discusses the effect of noise, delay in the transmission of the signals and loss of information in the communication system.

The paper is organized as follows. Section 2 describes the frequency control schemes of wind turbines, SPVGs and ESSs. Section 3 presents a fundamental-frequency model of the PLL that allows considering numerical issues for the estimation of the frequency. Section 4 presents the three strategies to retrieve the input signal of the DER frequency controllers considered in the paper, whereas Section 5 discusses in detail the case study. Finally, Section 6 duly draws conclusions and outlines future work.

2. PRIMARY FREQUENCY CONTROL OF DERS

This section briefly outlines the most common frequency regulation techniques for wind turbines, SPVG and ESSs in Subsections 2.1, 2.2 and 2.3, respectively.

2.1 Wind Turbines

Figure 1 depicts one of the most common frequency control techniques applied to wind turbines [Ramtharan et al. (2007); Ekanayake and Jenkins (2004); Morren et al. (2006); Cerqueira et al. (2017)]. The approach consist of varying the output signal of the MPPT, based on the deviation of a measured frequency $\hat{\omega}$ with respect to a reference ω^{ref}. The controller includes two parallel and complementary channels to regulate the frequency deviations (droop control) and/or the Rate of Change of Frequency (RoCoF control). A low-pass filter (LPF) with time constant T_r is included to filter out noises and possible numerical errors of the frequency error, and to inhibit steady-state signals from the controller, thus preventing the machine from stalling.

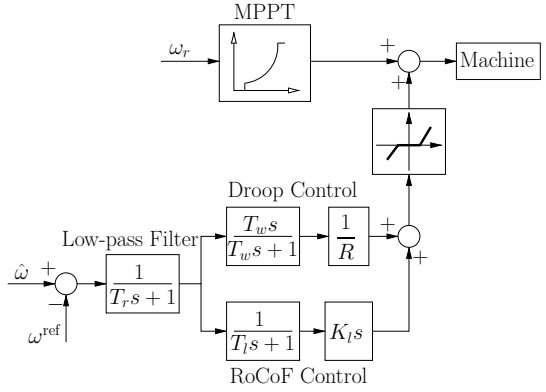

Fig. 1. Scheme of the droop and RoCoF controllers coupled to the MPPT of a wind turbine.

2.2 Solar Photo-Voltaic Generation

The scheme of the frequency control of SPVG is shown in Fig. 2 [Tamimi et al. (2011); Ko et al. (2007); Fernandez-Bernal et al. (2002)]. Due to the similarities between the connection of SPVGs and wind turbines with the grid, their control schemes also show a relevant resemblance. In this case, a droop control composed of droop gain and a LPF is implemented. The output signal is then added to the MPPT reference power, and processed by a PI regulator, which generates the d-axis component of the reference current input signal of the SPVG converter.

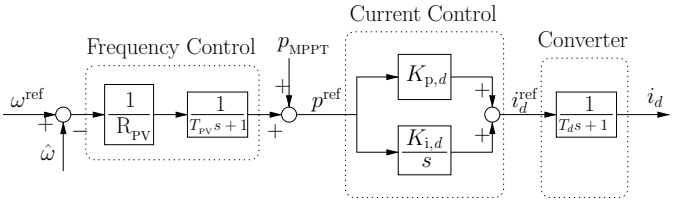

Fig. 2. Scheme of the frequency control of SPVGs.

2.3 Energy Storage Systems

Figure 3 depicts the active power control scheme of a simplified ESS, aimed at regulating a given measured frequency $\hat{\omega}$ [Pal et al. (2000)]. The controller is composed of a PI regulator coupled with a LPF. In this case, the droop gain is emulated as the integral deviation $H_{\text{d},P}$.

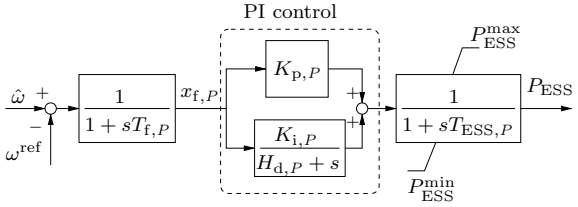

Fig. 3. Scheme of the frequency control of an ESS.

3. PHASE-LOCKED LOOP

A common component of the power electronic converters used to connect the DERs to the grid is the PLL. While the primary goal of PLLs is the synchronization of the converters with the grid, they can also provide a estimation of the frequency at the bus of connection. There exist a large variety of PLL configurations designed for power electronic converters, being the synchronous reference frame (SRF)–PLL one of the most common due mainly to its simplicity [Nicastri and Nagliero (2010); Ortega and Milano (2017b)]. A fundamental-frequency model of a SRF–PLL is shown in Fig. 4.

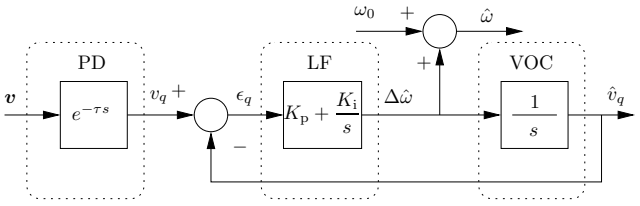

Fig. 4. Scheme of the SRF–PLL. ω_0 is the system reference frequency.

This configuration includes the following components: (i) a phase detector (PD) that measures the bus voltage phasor $\boldsymbol{v}$ at the point of connection of the PLL, and retrieves the information of the q-axis component of the voltage v_q; (ii) the loop filter (LF), which takes the error ϵ_q between the measured v_q and the one estimated by the SRF–PLL, $\hat{v}_q$, and is generally implemented as a PI regulator; and

(iii) the voltage oscillator control (VOC), which takes the estimation of the bus frequency deviation $\Delta\hat{\omega}$ and provides the estimation of $\hat{v}_q$.

The main issues related to the estimation of the bus frequency by using SRF–PLLs are that they inherently include delays in the measured signal, and that the derivation of $\hat{v}_q$ in the LF amplifies the noise, and to numerical issues during discontinuous events such as line outages, faults, etc.

4. STRATEGIES TO DEFINE THE FREQUENCY CONTROL SIGNAL

This paper compares three different strategies to generate the input signal of the frequency controllers of DERs, namely centralized, decentralized, and average. The three strategies are illustrated in Fig. 5. Note that we do not use the terms *centralized* and *decentralized* with the conventional meaning that they have in control applications. In this paper, the frequency controllers of DERs are local. *Centralized* and *decentralized* and *average* refer only to the strategy to define the input signals of such controllers.

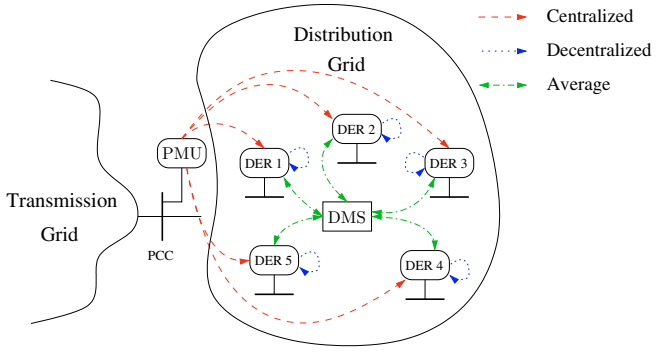

Fig. 5. Illustration of the three strategies to retrieve the frequency control input signal.

Centralized: In this strategy, the frequency at the point of common coupling (PCC) between the transmission (TG) and distribution grids (DG) is measured by means of, e.g., a phasor measurement unit (PMU), and then the signal is sent to every DER installed. As all DERs use the same frequency signal in their regulators, a good overall control performance can be expected from this strategy. However, it is also characterized by a certain communication delay related to the measure and dispatch of the frequency signal that can deteriorate such a performance. Moreover, as the overall frequency control relies on only one measure, it is desirable to have a redundancy by means of, e.g., a second PMU connected at the PCC, to avoid the loss of all regulation capability in case of possible PMU malfunctions.

Decentralized: The second strategy considers that all DERs measure the frequency at their own bus of connection, by means of the SRF–PLLs included in their power electronic converters, in a decentralized manner. The main advantage of this strategy is that it does not include any communication delay in the process, as measurement and control is done locally. On the other hand, this strategy does not provide any form of *coordination* between DERs. Moreover, while the frequency variations estimated at every DER bus of a DG should be the same, this estimation can significantly differ from bus to bus during transients due mainly to the numerical issues that derive from the numerical derivation of v_q.

Average: In the last strategy described in this Section, the SRF–PLL frequency estimations from every DER bus are sent and collected by a Data Management System (DMS) located generally within the DG. The DMS then computes the average value of all the signals, and then this average is sent back to every DER. This strategy shares its main advantage with the centralized approach, as all DERs regulate the frequency using the same signal. Moreover, averaging process of such a signal can allow reducing the impact of the spikes and other numerical issues present in the measured signals, as well as that of losing one or more of the measurements. However, as this strategy is based on a bidirectional communication channel, one must carefully consider the related delays.

5. CASE STUDY

This paper considers a modified version of the well-known WSCC 9-bus, 3-machine test system depicted in Fig. 6 for simulations (see [Sauer and Pai (1998)]). To compare the different strategies to retrieve the input signals of the frequency regulators of DERs in a DG, the load at bus 6 has been replaced with a 8-bus, 38 kV distribution system (see [Murphy and Keane (2017)]). For all scenarios included in this section, primary voltage and frequency regulations are considered.

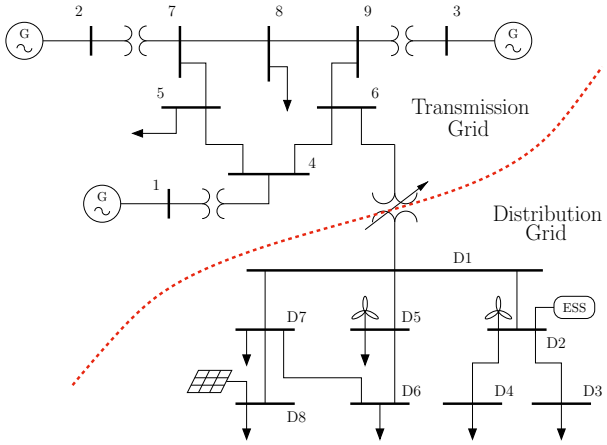

Fig. 6. Modified WSCC 9-bus, 3-machine system where the load at bus 6 has been substituted with a 8-bus, 38 kV distribution system.

This modified version of a small Irish DG includes both radial and meshed configurations, and is composed of eight buses and lines, six loads, two wind power plants, one solar PV plant, and one ESS. The operating nominal voltage of buses D1–D8 is 38 kV, and the DG is connected through an under-load tap changer (ULTC) type step down transformer with the TG. The total active and reactive power consumed by the loads of the DG is 0.578 MW and 0.117 MVar, respectively. The active power generation at the initial operating point of the wind power plants at buses D2 and D5, and of the solar PV plant at

bus D8 are of 15 MW each. The power rate of the ESS at bus D2 is 10 MW. For the short time scales considered in this paper, energy limits of the ESS are neglected.

Due to the presence of DERs, the total load level of the DG is lower than the original load connected at bus 6 of Fig. 6. Therefore, one needs to reduce accordingly the active power generation of the synchronous machines in order to keep the power balance at the initial operating point.

Each DER at buses D2, D5 and D8 includes a SRF–PLL that retrieves the bus frequency signal.[1] Identical gains $K_\mathrm{p} = 0.2$ and $K_\mathrm{i} = 0.05$ of the LF of the PLL scheme described in Section 3 have been used for all DERs. In this paper, the frequency signals of the regulators of the wind power plant and the ESS at bus D2 are generated by a single PLL. One can also consider the possibility of having two different PLLs measuring the frequency of bus D2. While this will lead to little differences for the decentralized strategy, as both signals will be very similar if both PLLs are identical, it can have an impact for the average strategy, as one more signal will be used in the computation of the averaged frequency.

Two main scenarios have been considered in this section, as follows. First, Subsection 5.1 studies and compares the impact of noises and delays of the frequency signals for the three strategies described in Section 4. Then, the robustness of each strategy against the loss of one of the PLL measures is analyzed in Subsection 5.2.

For both scenarios, the contingency considered is a three-phase fault at bus 7 at $t = 1$ s, cleared after 150 ms by means of the opening of the line connecting buses 5 and 7.

5.1 Impact of noise and communication delays

In this scenario, noise is introduced at the bus voltage angle of every bus of the DG. This noise accounts for possible unbalances, proximity of the loads, harmonics of the power electronic devices, etc. The Ornstein-Uhlenbeck's process with Gaussian Distribution is used to model the noise [Milano and Zárate-Miñano (2013)]. Same parameters are used for all buses D1-D8 to generate the noise profiles.

The delays associated to the processing and communication of the frequency control signals are also taken into account. To this aim, depending on the strategy used to retrieve such signal, different values of the time delay τ are assigned accordingly. The default τ used for every PLL is 5 ms, to account for the time needed to perform the signal measurement and variable transformation. This value is thus used for the decentralized strategy in the remainder of this Subsection.

The scenario where communication delays are neglected is first studied (i.e., $\tau = 5$ ms for all PLL for the three control signal retrieval strategies). The performance of the system for the different strategies are compared by observing the frequency at bus 6, i.e., the PCC of the TG and the DG, as depicted in Fig. 7. Such trajectories are obtained by applying the FD formula outlined in Appendix A, which provides a highly accurate frequency estimation that is free from noise, delays and numerical issues.[2] Figure 7 also includes, as a reference for the comparison, the *ideal* response obtained by using the FD signal as the input signal of the frequency regulators.

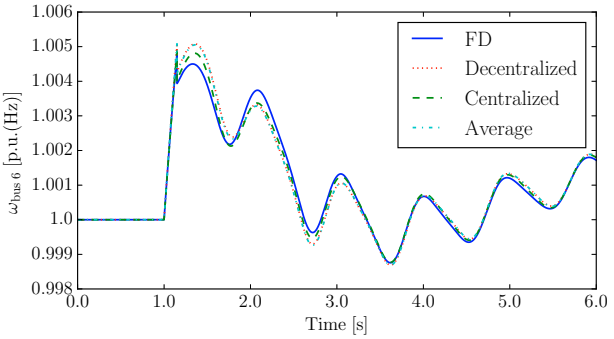

Fig. 7. Frequency of bus 6 after a three-phase fault. No communication delays are considered.

All three PLL-based responses are worse than the one based on the FD, as they show larger frequency deviations at the first instants after the contingency, even for the scenario where no communication delays are considered. This is better visible in Fig. 8, where the absolute errors with respect to the FD-based trajectory, ϵ_ω, are represented.

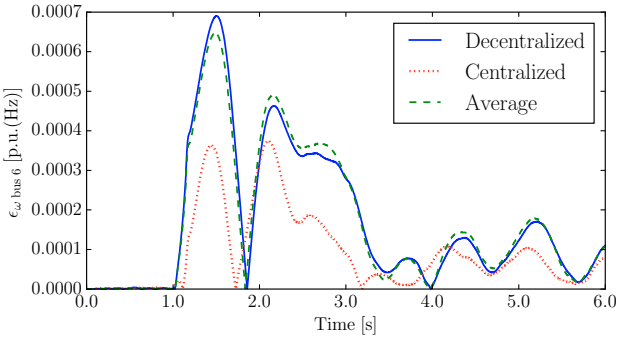

Fig. 8. Absolute error of the frequency at bus 6 after a three-phase fault. No communication delays are considered.

The centralized strategy (which takes the measure from bus D1) shows a better response than the other two, which show a fairly similar profile. This is because the signal is measured at the bus that is closest to the TG, thus the least affected by voltage fluctuations and, in turn, shows lower "spikes" derived from the numerical derivative of the bus voltage phasor during the fault, and few instants after the line outage.

This observation is confirmed by Fig. 9, where the PLL measures of the DER buses D2, D5 and D8, as well as their averaged signal, are represented. The farther is the PLL device from the PCC, the more sensitive to numerical issues is the generated signal. From Fig. 9, one can also justify why the decentralized and the average strategies are similar. In fact, by averaging the signals one can reduce the impact of the worst signal (bus D8), but also one cannot

[1] In the remainder of this document, the acronym PLL will be used to refer to the SRF–PLL

[2] Note that, while the FD formula can provide an *ideal* frequency estimation in simulations, it is impractical, as one requires the knowledge of all synchronous machine rotor speeds. Hence the utilization of the PLL-based strategies proposed in this paper.

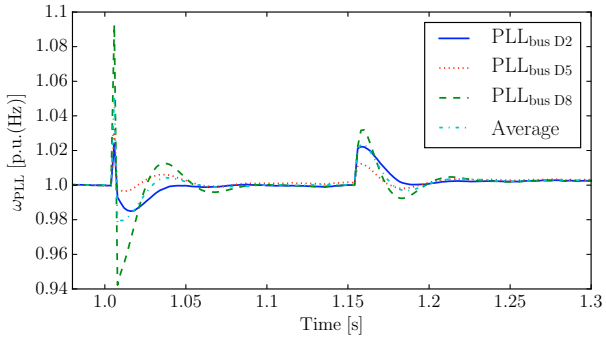

Fig. 9. Frequency signals measured with the different PLLs, and their average. No communication delays are considered.

benefit from the better quality of the signals generated by the PLLs at buses D2 and D5.

The impact of noise on the performance of the frequency controllers is negligible for all cases, as such a noise is properly filtered out by the LPFs of the regulators.

The impact of communication delays are next studied. To this aim, it is assumed that the time needed to i) send the measured signal from bus D1, and ii) to retrieve the three PLL signals from buses D2, D5, and D8, compute and send the averaged signal back to the regulators is 20 ms for both cases. Therefore, $\tau = 5$ ms for the decentralized strategy, and $\tau = 25$ ms for both the centralized and the average strategy. Note that the 5 ms delay needed to measure and process the signal is still taken into account. The generated ϵ_ω of trajectories of the frequency at bus 6 are depicted in Fig. 10.

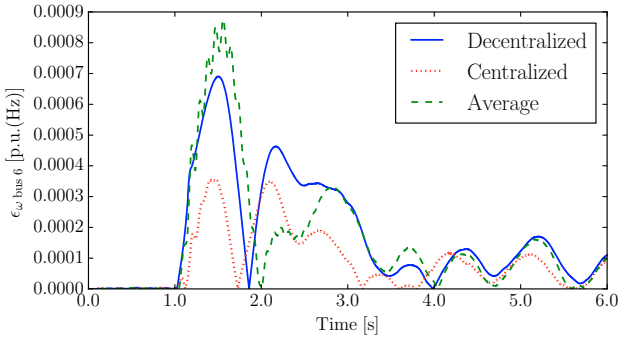

Fig. 10. Absolute error of the frequency at bus 6 after a three-phase fault. Communication delay is 20 ms.

The performance of the average strategy deteriorates due to the inclusion of the communication delay. Note also that, due to the larger delay, the frequency controllers of the DERs also insert frequency oscillations of small amplitude and with a period of about 0.1 s. The centralized strategy, on the other hand, does not appear to be affected by such a delay. However, if the time required to send the signal from bus D1 to the DERs increases similar *high-frequency* oscillations are observed, as shown in Fig. 11, where a communication delay of 55 ms for the centralized strategy is included (i.e., $\tau = 60$ ms). Figure 11 also shows the unstable response of the average strategy for a communication delay of 35 ms.

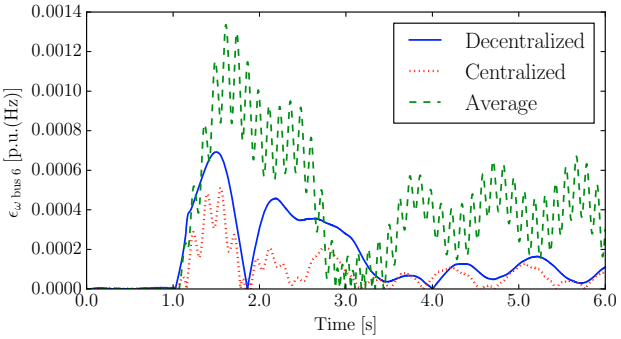

Fig. 11. Absolute error of the frequency at bus 6 after a three-phase fault. Communication delays are 35 and 55 ms for the average and centralized strategies, respectively.

5.2 Robustness Against Loss of Information

In this scenario, the robustness of the three strategies against the loss of a measurement signal is studied. To this aim, the PLL from one DER bus is assumed to malfunction when trying to send its measurement to both the decentralized and the average strategies. As the centralized strategy only depends on the single measurement of bus D1, it is assumed to have a redundancy of such a measurement in case of signal loss, to prevent that all frequency control from the DERs is disabled. Therefore, the performance of the centralized strategy is the same as that shown in Subsection 5.1 above.

Figure 12 shows the ϵ_ω of the three strategies when the PLL at bus 8 fails to retrieve/send its frequency measurement. The total delays τ assumed are again 5 ms for the decentralized strategy and 25 ms for the centralized and average ones.

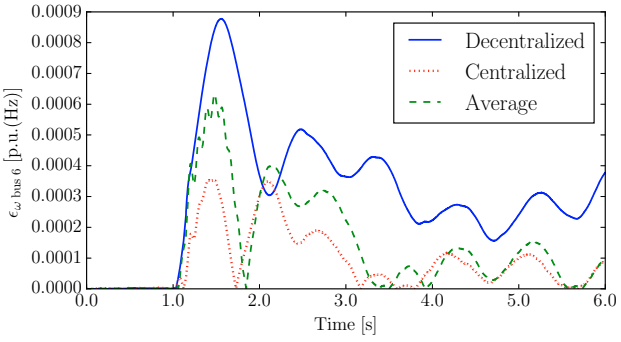

Fig. 12. Absolute error of the frequency at bus 6 after a three-phase fault. The frequency signal of bus D8 is lost for the average and decentralized strategies.

It can be seen that, for the decentralized strategy, the error ϵ_ω increases by about 20% with respect to that of Fig. 10 in the first swing after the contingency. Moreover, such ϵ_ω is considerably higher than that of the other strategies throughout the rest of the simulation. On the other hand, the loss of the D8 measurement improves the performance of the average strategy by reducing ϵ_ω during the first instants after the contingency by about 30%. This interesting result is justified by the fact that the signal from the PLL of bus D8 is also the most affected

by the spikes as shown previously in Fig. 9. Therefore, the resulting average signal shows a better accuracy, thus leading to a better performance of the DER frequency regulator.

6. CONCLUSION

The paper compares the performance of three strategies to obtain the input signal of a variety of primary frequency regulators of DERs, namely centralized, decentralized and average.

Simulation results indicate that, while the centralized strategy shows a better overall performance, it highly depends on the associated signal communication delays. To avoid the loss of all regulation capability in case of malfunctions of the measurement device, a redundancy of such a measure is desirable. The decentralized strategy works reasonably well, and it does not include any form of communication delay. However, its overall performance can be highly deteriorated in case of loss of any of the frequency measures. The average strategy shows a good robustness against the loss of measurement signals without the need of redundant measures. It naturally filters out the largest spikes and other numerical issues of the measures during transients. Similarly to the centralized strategy, its performance highly depends on the communication delays.

Based on these results, future work will focus on the improvement of the average strategy by means of the identification of the areas within the distribution grid with high density of DERs installed, with the aim of minimizing the related communication delays.

Appendix A. FREQUENCY DIVIDER

The *Frequency Divider* (FD) has been originally proposed by the authors in [Milano and Ortega (2017)]. The FD is based on the augmented admittance matrix of the network and consists of a linear relationship between local bus frequency variations and the deviation of synchronous machine rotor speeds, as follows:

$$\mathbf{0} = \mathbf{B}_{BB} \cdot \Delta\boldsymbol{\omega}_B + \mathbf{B}_{BG} \cdot \Delta\boldsymbol{\omega}_G \tag{A.1}$$

where $\Delta\boldsymbol{\omega}_B$ are the bus frequency deviations; $\Delta\boldsymbol{\omega}_G$ are the synchronous machine rotor speed deviations; $\mathbf{B}_{BB}$ is the extended network susceptance matrix with inclusion of the internal reactances of the synchronous machines; and $\mathbf{B}_{BG}$ is incidence susceptance matrix at the bus where generators are connected to the network.

The expression (A.1) has been thoroughly discussed and validated in [Milano and Ortega (2017); Ortega et al. (2017)] and is accurate for standard transient stability analysis of power systems.

REFERENCES

Cerqueira, J., Bruzzone, F., Castro, C., Massucco, S., and Milano, F. (2017). Comparison of the dynamic response of wind turbine primary frequency controllers constraints. In *IEEE PES General Meeting*, 1–5.

Ekanayake, J. and Jenkins, N. (2004). Comparison of the response of doubly fed and fixed-speed induction generator wind turbines to changes in network frequency. *IEEE Trans. on Energy Conversion*, 19(4), 800–802.

Etherden, N., Vyatkin, V., and Bollen, M.H.J. (2016). Virtual power plant for grid services using IEC 61850. *IEEE Trans. on Industrial Informatics*, 12(1), 437–447.

Fernandez-Bernal, F., Rouco, L., Centeno, P., Gonzalez, M., and Alonso, M. (2002). Modelling of photovoltaic plants for power system dynamic studies. In *5th Int. Conf. on Power System Management and Control*, 341–346.

Ko, H.S., Yoon, G.G., and Hong, W.P. (2007). Active use of DFIG-based variable-speed wind-turbine for voltage regulation at a remote location. *IEEE Trans. on Power Systems*, 22(4), 1916–1925.

Koraki, D. and Strunz, K. (2018). Wind and solar power integration in electricity markets and distribution networks through service-centric virtual power plants. *IEEE Trans. on Power Systems*, 33(1), 473–485.

Milano, F. and Zárate-Miñano, R. (2013). A systematic method to model power systems as stochastic differential algebraic equations. *IEEE Trans. on Power Systems*, 28(4), 4537–4544.

Milano, F. and Ortega, Á. (2017). Frequency divider. *IEEE Trans. on Power Systems*, 32(2), 1493–1501.

Morren, J., de Haan, S.W.H., Kling, W.L., and Ferreira, J.A. (2006). Wind turbines emulating inertia and supporting primary frequency control. *IEEE Trans. on Power Systems*, 21(1), 433–434.

Murphy, C. and Keane, A. (2017). Local and remote estimations using fitted polynomials in distribution systems. *IEEE Trans. on Power Systems*, 32(4), 3185–3194.

Nicastri, A. and Nagliero, A. (2010). Comparison and evaluation of the PLL techniques for the design of the grid-connected inverter systems. In *IEEE Int. Symposium on Industrial Electronics*, 3865–3870.

Ortega, Á. and Milano, F. (2017a). Modeling, simulation, and comparison of control techniques for energy storage systems. *IEEE Trans. on Power Systems*, 32(3), 2445–2454.

Ortega, Á., Milano, F., Musa, A., Toma, L., and Preotescu, D. (2017). Definition of frequency under high dynamic conditions. Technical report, RESERVE Consortium. Deliverable 2.1, available at: www.re-serve.eu.

Ortega, Á. and Milano, F. (2017b). Impact of frequency estimation for VSC-based devices with primary frequency control. In *Proceedings of the IEEE PES ISGT Europe*, 1–6.

Pal, B.C., Coonick, A.H., Jaimoukha, I.M., and El-Zobaidi, H. (2000). A linear matrix inequality approach to robust damping control design in power systems with superconducting magnetic energy storage device. *IEEE Trans. on Power Systems*, 15(1), 356–362.

Ramtharan, G., Ekanayake, J.B., and Jenkins, N. (2007). Frequency support from doubly fed induction generator wind turbines. *IET Renewable Power Generation*, 1(1), 3–9.

Sauer, P.W. and Pai, M.A. (1998). *Power System Dynamics and Stability*. Prentice Hall, Upper Saddle River, NJ.

Tamimi, B., Cañizares, C., and Bhattacharya, K. (2011). Modeling and performance analysis of large solar photovoltaic generation on voltage stability and inter-area oscillations. In *IEEE PES General Meeting*, 1–6.